Carbohydrate Polymers 86 (2011) 1705–1711

Contents lists available at ScienceDirect

Carbohydrate Polymers

journal homepage: www.elsevier.com/locate/carbpol

Structural characteristics of a hyperbranched acidic polysaccharide from the stems of *Ephedra sinica* and its effect on T-cell subsets and their cytokines in DTH mice

Haixue Kuang*, Yonggang Xia, Jun Liang, Bingyou Yang, Qiuhong Wang, Xinguo Wang

Key Laboratory of Chinese Materia Medica (Heilongjiang University of Chinese Medicine), Ministry of Education, Harbin 150040, China

ARTICLE INFO

Article history:
Received 21 May 2011
Received in revised form 25 June 2011
Accepted 1 July 2011
Available online 7 July 2011

Keywords:
Ephedra sinica Stapf
Polysaccharides
Structural characteristics
Delayed-type hypersensitivity
Immunosuppressive effects

ABSTRACT

An acidic hetero-polysaccharide (ESP-B4) was acquired from the stems of *Ephedra sinica*. Its structure was characterized by periodate oxidation, Smith degradation, partial acid hydrolysis, methylation analysis combined with HPCE, GC–MS and FT-IR spectra. The results indicated that ESP-B4 contained a repeating unit of [→4)-Gal*p*A-(1→2)-Rha*p*-(1→] as hairy region, substituted by arabinose, xylose, galactose, glucose, mannose and glucuronic acid. To better understand the mechanism of bioactivity for this compound, the quantities of ESP-B4 was further enriched by ion exchange and gel filtration chromatography. Immunological tests in vivo showed that ESP-B4 exhibits compelling immunosuppressive effects by hematoxylin and eosin staining, enzyme-linked immunosorbent assay and flow cytometric analysis. The mechanism of action might be attributed to its inhibition of IL-2 and IL-4 levels in serum, and also effectively suppressed the ratio of $CD4^+/CD8^+$ in serum of T cell mediated delayed-type hypersensitivity mice. The results suggest that ESP-B4 could be a valuable lead material for immunosuppressive drug development.

1. Introduction

As a traditional Chinese medicine, *Ephedra sinica* Stapf (Mahuang), has been used to treat various diseases such as asthma, pneumonia, bronchitis, hay fever and colds for a long time in China (Cheng, Zhu, & Xu, 2001; Comar & Kirby, 2005). Polysaccharides, as primary extracts from *E. sinica*, also have been confirmed to be an important contributor to immunosuppressive effects (Ding, Shi, Cui, Wang, & Wang, 2006; Kuang, Xia, Yang, Wang, & Wang, 2011; Xia, Liang, Yang, Wang, & Kuang, 2010; Xia et al., 2011a). In previous works, several polysaccharides possessing immunosuppressive effects have been purified in our laboratory from the stems of *E. sinica* (Kuang et al., 2011). ESP-B4 was isolated by a series of purified steps including DEAE-cellulose 52 column and Sephacryl S-400, and has been determined to be a homogeneity with a relative molecular weight of more than 2.0×10^6 Da (determined by HPLC). ESP-B4 was a typical acidic hetero-polysaccharide and consisted of xylose, arabinose, glucose, rhamnose, mannose, galactose, glucuronic acid and galacturonic acid, and their corresponding molar ratios were 1.0:4.5:1.0:2.0:1.0:5.5:1.5:50.0 by high performance capillary electrophoresis (HPCE) based on pre-column derivatization with 1-phenyl-3-methyl-5-pyrazolone (PMP) (Xia et al., 2011b). Besides, ESP-B4 has been confirmed to possess an ability of inhibitory effect on splenocyte proliferation and its branches are extremely important for the expression of the inhibitory effect (Kuang et al., 2011).

According to the literature report, many of the bioactivities of polysaccharides from herb plants have been shown to have a relationship with complex branched structures (Kuang et al., 2011; Sun et al., 2010; Tong, Liang, & Wang, 2008), so the elucidation of molecular fine structural characteristics of polysaccharides is quite necessary for understanding the mechanism of physiological activity and clarifying the structure–activity relationships. However, up to now, little attention has been given to the elucidation of polysaccharides present in the stem of *E. sinica*. Taking this into account, it becomes necessary to investigate the chemical nature of the active principle in *E. sinica*. Therefore, the present work is devoted to further clarification of the detailed structural features of the polysaccharide ESP-B4 from *E. sinica* using periodate oxidation, Smith degradation, partial acid hydrolysis and methylation analysis combined with HPCE, GC–MS and FT-IR spectra. Moreover, we provided evidence, for the first time, to demonstrate the immunosuppressive effect of ESP-B4 on T lymphocytes subsets and cytokines in T cell mediated delayed type hypersensitivity (DTH) mice. The in-depth study of its immunosuppressive mechanisms is bound to provide some useful information on its promising therapeutic application.

* Corresponding author. Tel.: +86 45182193001; fax: +86 45182110803.
E-mail address: hxkuang@hotmail.com (H. Kuang).

0144-8617/$ – see front matter © 2011 Elsevier Ltd. All rights reserved.
doi:10.1016/j.carbpol.2011.07.001

2. Experimental

2.1. Materials and reagents

2,4-Dinitrofluorobenzene (DNFB) was from PharMingen products (SanDiego, CA). D-mannose (Man), L-rhamnose (Rha), D-glucose (Glc), D-galactose (Gal), L-arabinose (Ara), D-xylose (Xyl), D-glucuronic acid (GlcUA), D-galacturonic acid (GalUA), sulfuric acid (H_2SO_4), DEAE Sepharose Fast Flow, Sephacryl S-400 HR, Sephacryl S-300 HR and Sephacryl S-100 HR were from the Pharmacia Co. (Sweden). DEAE-52 was purchased from Whatman International Ltd. (Maidstone, Kent, UK). All other chemicals were of the highest grade available.

2.2. Plant materials and preparation of ESP-B4

The dry stems of *E. sinica* were collected in March 2007 from Datong of Shanxi Province, China and identified by Prof. Zhenyue Wang of Heilongjiang University of Chinese Medicine. The voucher specimen (20070016) was deposited at Herbarium of Heilongjiang University of Chinese Medicine, Harbin, P.R. China. Isolation followed by purification of the acidic polysaccharide ESP-B4 from stems of *E. sinica* was performed as described earlier (Kuang et al., 2011).

2.3. IR spectral analysis of ESP-B4

The structural characteristics of the ESP-B4 were determined using a Fourier-transform IR spectrophotometer (Shimadzu FTIR-8400S). The purified polysaccharides were ground with KBr powder and then pressed into pellets for transform IR spectral measurement in the frequency range of 4000–400 cm^{-1}.

2.4. Periodate oxidation and Smith degradation studies

ESP-B4 (10 mg) was incubated with 20 mL of 15 mmol sodium metaperiodate for 5 days at 4 °C in the dark. The production of formic acid and consumption of periodate were periodically analyzed by titration with 0.01 M NaOH and colorimetry. Formic acid production was titration with spectrophotometric method. Excess $NaIO_4$ was decomposed by the addition of 50 μL of ethylene glycol. The solution was dialyzed against distilled water for 24 h and treated with $NaBH_4$ (40 mg) for 24 h at 25 °C. The product was then successively adjusted to pH 5 with 0.1 M acetic acid, dialyzed against water and, acetylated; the resulting mixture was analyzed by GC–MS.

2.5. Partial acid hydrolysis

ESP-B4 (200 mg) was hydrolyzed with 0.1 M TFA (3 mL) for 6 h at 100 °C, and TFA was removed in vacuum by addition of methanol repeatedly. The hydrolysis sample was dialyzed with distilled water for 48 h in a dialysis sack (cut-off, M_w = 3500 Da), and then diluted the solution in the sack with ethanol. After hydrolysis, the precipitate (a) and supernatant in the sack (b) and the fraction out of sack (c) were dried, respectively. A similar procedure was used with 0.4 M TFA and 0.8 M TFA for the above steps after 0.4 M TFA and 0.8 M TFA treated. Composition analysis was performed as described earlier (Kuang et al., 2011; Xia et al., 2011b). Our experimental protocols are shown as in Fig. 1. Chemical composition of ESP-B4-a∼ESP-B4-h can be seen in Table 1.

2.6. Methylation analysis

ESP-B4 (5 mg) were methylated three times with powdered sodium hydroxide and methyl iodide in dimethyl sulphoxide solution by the method of references (Ghosh et al., 2008; Mondal et al., 2008; Ojha et al., 2008), and the resulting partially methylated products were hydrolyzed, reduced, acetylated and analyzed by GC–MS as described previously. The partially methylated alditol acetates were identified by their relative retention times on GC and fragment ions in EI-MS, and the molar ratios were estimated from the peak areas and response factors.

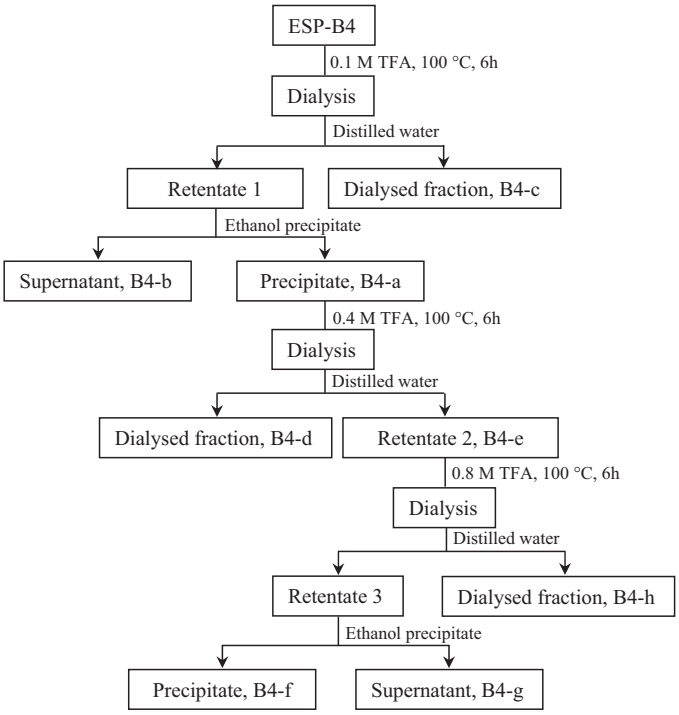

Fig. 1. Scheme for partial acid hydrolysis of ESP-B4.

2.7. Animals and DNFB-induced delayed type hypersensitivity reaction (DTH)

Male BALB/c mice, aged 6–8 weeks (18–22 g) were obtained from Experimental Animal Center of Heilongjiang University of Chinese Medicine (Harbin, China). They were maintained with free access to pellet food and water in plastic cages at 21 ± 2 °C, 60 ± 5 humidity, and kept on a 12 h light/dark cycle. Animal welfare and experimental procedures were carried out strictly in accordance with the guide for the care and use of laboratory animals (The Ministry of Science and Technology of China, 2006) and the related ethical regulations of our university. All efforts were made to minimize animal's suffering and to reduce the number of animals used.

DNFB-DTH assay was performed as our previously described (Kuang et al., 2011). In brief, on days 1 and 2, BALB/c mice were sen-

Table 1
HPCE analysis results of partial acid hydrolysis products.

Fractions	Molar ratios (mol%)							
	Xyl	Ara	Glc	Rha	Man	Gal	GlcUA	GalUA
ESP-B4	1.5	6.8	1.5	3.0	1.5	8.3	2.3	75.2
ESP-B4-a	3.1	7.2	1.0	3.7	1.4	11.5	1.9	70.3
ESP-B4-b	–	9.5	–	–	–	5.0	–	85.6
ESP-B4-c	4.5	13.3	–	–	4.5	16.0	2.5	59.1
ESP-B4-d	6.4	29.6	–	7.7	4.1	17.2	2.6	32.4
ESP-B4-e	3.3	–	–	4.5	1.8	14.0	2.9	73.5
ESP-B4-f	–	–	0.6	4.5	0.4	–	1.5	93.1
ESP-B4-g	–	–	0.7	4.7	7.8	9.7	5.5	71.7
ESP-B4-h	0.2	1.6	0.9	3.9	1.7	8.6	5.1	78.1

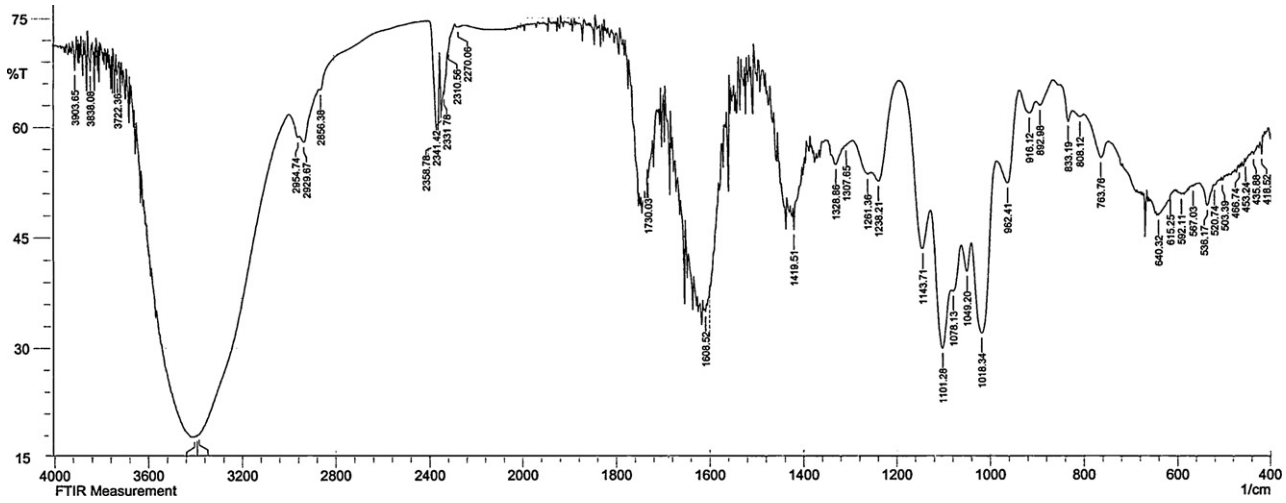

Fig. 2. FT-IR profile of ESP-B4.

sitized by skin painting on each shaved abdomen with 20 μL of 5% DNFB dissolved in acetone–olive oil (4:1). Five days later, they were challenged on both sides of their right ear with 10 μL of 5% DNFB. The DTH reaction was evaluated by the increase in ear thickness measured with the engineer's micrometer 22 h after the challenge.

2.8. Effect of ESP-B4 on $CD3^+$, $CD4^+$ and $CD8^+$ T cell in DTH mice

Anti-mouse CD4(L3T4)-FITC, CD8(Ly-2)-PreCP and CD3-PE for flow cytometric analysis were purchased from Becton Dickinson (BD) PharMingen (San Diego, CA). They were analyzed with a FACScan flowcytometer (Becton Dickinson, San Jose, CA) and the data were processed using Cell Quest software (Becton Dickinson).

2.9. Effect of ESP-B4 on serum IL-2, IL-4 and γ-IFN in DTH mice

Levels of Interleukin-2 (IL-2), Interferon-γ (IFN-γ) and Interleukin-4 (IL-4) in serum of different groups were measured using commercially available enzyme-linked immunosorbent assay (ELISA) kits according to the test protocols. ELISA kits for IL-2, IFN-γ and IL-4 (anti-mouse) were the products of Jingmei Biotech, Shenzhen, China. We collected the serum and stored them at −20 °C.

2.10. Ear tissue histopathology

All the mice were sacrificed and their right ears were removed. Samples were fixed in 10% polyoxymethylene for histological assessment of the lesions by hematoxylin and eosin (HE) staining.

2.11. Statistical analysis

Data were expressed as the mean standard deviation of the means (S.D.) and statistical analysis was performed by paired samples *t*-test using SPSS 16.0 to evaluate the significance of differences between groups.

3. Result and discussion

3.1. Preparation of ESP-B4

The acidic polysaccharide named ESP-B4 has been isolated and purified from the stems of *E. sinica* as described earlier (Kuang et al., 2011; Xia et al., 2011b). As a result, 1.0 g of ESP-B4 was obtained for the following experiments. The sugar composition of ESP-B4 was listed in Table 1. ESP-B4 showed only one symmetrical peak on high performance gel-permeation chromatography. Its molecular mass was estimated to be more than 2.0×10^6 Da in reference to standard dextrans. No absorption at 280 nm and a negative response to the Lowry method (Bensadoun & Weinstein, 1976) confirmed that ESP-B4 did not contain protein.

3.2. Structural characteristics of ESP-B4

3.2.1. FT-IR spectral analysis

The FT-IR spectrum of ESP-B4 is presented in Fig. 2. The attributions of the main absorptions are characteristic of glycosidic structures and are related to CO stretching (1101 cm^{-1}, 1018 cm^{-1}, and 1049 cm^{-1}) and anomeric C_1H group vibration (833 cm^{-1} and 916 cm^{-1}) (Li, Fan, & Ding, 2011; Sun et al., 2010). Moreover, the characteristic absorptions at 833 cm^{-1} and 916 cm^{-1} in the IR spectra indicated that and α and β-configurations were simultaneously. Stronger bands occurring between 1730 cm^{-1} and 1608 cm^{-1} are derived from the ester carbonyl (–COOR) groups and carboxylate ion stretching band (–COO–), respectively (Zhu et al., 2010). Further analysis of the FT-IR spectra revealed that a broad stretching intense characteristic peak at 3404 cm^{-1} for the hydroxyl group and a weak C–H stretching bond at 2929 cm^{-1}. The peak corresponding to pyranoid group at 892 cm^{-1} and 763 cm^{-1} indicated the existence of hexose (He et al., 2009; Qiao et al., 2010). This proved further the outcome obtained from HPCE and GC–MS analysis.

3.2.2. Partial acid hydrolysis

Partial degradation of polysaccharides by acid hydrolysis is based on the fact that some glycosidic linkages are more labile to acid than others. For example, linkages between neutral sugars are the most susceptible to acid hydrolysis; hence controlled acid hydrolysis is frequently used to remove neutral sugars (Dong, Yao, Fang, & Ding, 2007; Tong et al., 2008). To study the linkages between backbone and side chains of polysaccharide, the native polysaccharide ESP-B4 was partially hydrolyzed with 0.1, 0.4 and 0.8 M TFA by sequential hydrolysis (Fig. 1). Partial acid hydrolysis resulted in eight sub-fractions of ESP-B4. The sugar composition of fractions was given in Table 1 by HPCE. It showed that for the polymer fraction ESP-B4-a, its characteristics were close to the parent ESP-B4 with high branches, suggesting that a higher concentration of acid was necessary to be further partial acid hydrolysis. For the fractions ESP-B4-c, ESP-B4-d and ESP-B4-h, the sugar composition

presented in Table 1 showed that the neutral sugars (arabinose, galactose, mannose and xylose) were the main constituents except for rhamnose and galacturonic acid. These results confirmed that galacturonic acid and rhamnose present in the backbone can resist a higher concentration of acid, whereas the neutral sugars were attached to the side chains and easy to be hydrolyzed.

It is interesting that ESP-B4-f were also very close to the parent ESP-B4, the amount of arabinose, xylose, glucose, mannose, galactose and glucuronic acid decreased considerably compared with ESP-B4, whereas the amount of rhamnose and galacturonic acid increased, suggesting that linkages between two GalA sugars are more stable than aldobiuronic linkages (GalA-Rha) or pseudo-aldobiuronic (Rha-GalA) sugars and linkages between neutral sugars are most susceptible to acid hydrolysis. ESP-B4-f was composed of galacturonic acid (93.1%), rhamnose (4.5%), glucuronic acid (1.5%) and small amount of glucose and mannose (0.6% and 0.4%), suggesting the presence of a typical homogalacturonan and rhamnogalacturonan substituted by the side chains of mainly arabinose, xylose, galactose, glucose, mannose and glucuronic acid residues.

3.2.3. Periodate oxidation and Smith degradation

ESP-B4 (48 mg) was oxidized with 15 mmol $NaIO_4$ at room temperature in the dark for 3 days. The results from periodate oxidation showed that 0.314 mmol periodate was consumed and 0.149 mmol formic acid was produced per sugar residue, indicating the existence of small amount of monosaccharides which are 1→ linked or (1→6)-linked. The amount of consumed periodate was more than twice the yield of generated formic acid, indicating the existence of large amounts or 1→4 or (1→2)-linked sugar residue. The periodate-oxidized products were fully hydrolyzed and analyzed by HPCE and GC–MS analysis. The existence of a part of galactose, xylose, rhamnose, arabinose and galacturonic acid revealed that a part of galactose, xylose, arabinose, rhamnose and galacturonic acid residues was (1→3)-linked, (1→2,3)-linked, (1→2,4)-linked, (1→3,4)-linked, (1→3,6)-linked or (1→2,3,4)-linked that can not be oxidized. No glucose, mannose and glucuronic acid were observed, demonstrating that glucose, mannose and glucuronic acid were all linkages which can be oxidized by periodate. Smith degradation indicated that there was a small part of precipitation in the sack, demonstrated that the backbone of ESP-B4 can not be oxidized completely by HIO_4. Hence, it can be concluded that the linkages of backbone are (1→), (1→2), (1→6), (1→2,6), (1→4) and (1→4,6) that can be oxidized producing glycerin and erythritol detected out of sack.

3.2.4. Methylation analysis

Methylation analysis, the most popularly used method, is used to determine the sugar linkage of polysaccharides (Cui, 2005; Zhu et al., 2010). To measure the linked types of uronic acid, GalA and GlcUA were first reduced to Gal and Glc before methylation reaction. The reduced ESP-B4 was hydrolyzed with acid, converted into alditol acetates, and analyzed by GC–MS. As summarized in Table 2, the results showed the presence of 17 linked types, namely 2,3-Me_2-Ara*f*, 2-Me-Ara*f*, 2,3,4-Me_3-Xyl*p*, 2,4-Me_2-Xyl*p*, 3,4-Me_2-Rha*p*, 3-Me-Rha*p*, 2,3,4,6-Me_4-Glc*p*, 2,3,4,6-Me_4-Man*p*, 2,3,6-Me_3-Man*p*, 2,3,4,6-Me_4-Gal*p*, 2,4,6-Me_3-Gal*p*, 2,3,6-Me_3-Gal*p*, 2,4-Me_2-Gal*p*, 2,3-Me_2-Gal*p*, 2,3,6-Me_3-Gal*p*A, 2,6-Me_2-Gal*p*A and 2,3,6-Me_3-Glc*p*A in molar ratios of 3.6:2.8:1.0:0.2:1.2:2.8:1.7:0.8:0.8:2.2:1.1:1.5:2.6:1.8:55.2:18.6:2.1. These molar ratios agree with the overall monosaccharide composition described above. It showed that ESP-B4 was composed mainly of 1,4-linked Gal*p*A, 1,3,4-linked Gal*p*A, 1,2- and 1,2,4-linked rhamnose, 1,5-, 1,3,5-linked arabinose, terminal, 1,3-, 1,4-, 1,3,6-, and 1,4,6-linked galactose, as was commonly reported in pectic polysaccharide. Methylation analysis revealed that 2,3,6-tri-*O*-methyl-1,4,5 -tri-*O*-acetylgalactitol arising from the reduced 1,4-Gal*p*A was the main sugar component. The low amount (4.0%) of 3-*O*-methyl-1,2,4,5-tetra-*O*-acetyl-rhamnitol [→2,4)-Rha*p*-(1→] and 3,4-di-*O*-methyl-1,2,5-tri-*O*-acetyl-rhamnitol [→2)-Rha*p*-(1→] suggested that ESP-B4 contained the main part of homogalacturonan fragments as "smooth regions" (a linear chain of 1,4-Gal*p*A units) and certain amount of rhamnogalacturonan segments as "hairy regions". Regarding the rhamnosyl residues, the ratio 1.2:2.8 of 1,2- to 1,2,4-linked rhamnose indicated a total of 70% rhamnose residues in the backbone were substituted at O-4 position by side chains.

Table 2
Sugar linkage analysis of ESP-B4.

Sugar derivative	Mode of linkage	Mol%
2,3-Di-*O*-methyl-1,4,5-tri-*O*-acetyl-arabinitol	→5)-Ara*f*-(1→	3.6
2-*O*-Methyl-1,3,4,5-tri-*O*-acetyl-arabinitol	→3,5)-Ara*f*-(1→	2.8
2,3,4-Tri-*O*-methyl-1,5-di-O-acetyl-xylitol	α-Xyl*p*-(1→	1.0
2,4-Di-*O*-methyl-1,3,5-tri-O-acetyl-xylitol	→3)-Xyl*p*-(1→	0.2
3,4-Di-*O*-methyl-1,2,5-tri-O-acetyl-rhamnitol	→2)-Rha*p*-(1→	1.2
3-*O*-Methyl-1,2,4,5-tetra-O-acetyl- rhamnitol	→2,4)-Rha*p*-(1→	2.8
2,3,4,6-Tetra-*O*-methyl-1,5-di-*O*-acetylglucitol	Glc*p*-(1→	1.7
2,3,4,6-Tetra-*O*-methyl-1,5-di-*O*-acetylmannitol	Man*p*-(1→	0.8
2,3,6-Tri-*O*-methyl-1,4,5-tri-*O*-acetylmannitol	→4)-Man*p* -(1→	0.8
2,3,4,6-Tetra-*O*-methyl-1,5-di-*O*-acetylgalactitol	Gal*p*-(1→	2.2
2,4,6-Tri-*O*-methyl-1,3,5-tri-*O*-acetylgalactitol	→3)-Gal*p*-(1→	1.1
2,3,6-Di-*O*-methyl-1,4,5-tri-*O*-acetylgalactitol	→4)-Gal*p*-(1→	1.5
2,4-Di-*O*-methyl-1,3,5,6-tetra-*O*-acetylgalactitol	→3,6)-Gal*p*-(1→	2.6
2,3-Di-*O*-methyl-1,4,5,6-tetra-*O*-acetylgalactitol	→4,6)-Gal*p*-(1→	1.8
2,3,6-Tri-*O*-methyl-1,4,5-tri-*O*-acetylgalactitol	→4)-Gal*p*A-(1→	55.2
2,6-Di-*O*-methyl-1,4,5,6-tetra-*O*-acetylgalactitol	→3,4)-Gal*p*A-(1→	18.6
2,3,6-Tri-*O*-methyl-1,4,5-tri-*O* -acetylglucitol	→4)-Glc*p*A-(1→	2.1

The proportion of terminal, 1,3-, 1,4-, 1,3,6-, and 1,4,6-linked galactosyl was, respectively, in the ratio of 2.2:1.1:1.5:2.6:1.8. These results suggested that the galactan side chains contained a central core of 1,3-linked galactosyl residues, as 40.2% of the units were 1,3-linked, more than half of which (70.3%) were substituted at O-6 position (1,3,6-linked galactosyl). In addition, there was also a core of 1,4-linked galactosyl residues (35.9%), in which 54.5% of the units (1,4-linked galactosyl) were substituted at O-6 position (1,4,6-linked galactosyl). The low proportion of terminal galactosyl residues (23.9%) indicated that a part of the galactopyranan side chains were terminated by the arabinofuranose residues. The neutral side chains of arabinofuranosyl residues and galactopyranosyl residues were attached to the backbone at the O-4 position of rhamnopyranosyl residues.

3.3. Effect of ESP-B4 on T-cell subsets and cytokines in DNFB induced DTH reaction in mice

Delayed-type hypersensitivity (DTH) is a classic T cell-mediated immune reaction and plays an essential role in the pathogenesis and chronicity of various inflammatory disorders (Yin et al., 2008). The DTH reaction is based on a cell-mediated pathologic response involved in T cell activation and the production of many proinflammatory cytokines. Many immune-related diseases, such as multiple sclerosis, rheumatoid arthritis, contact hypersensitivity and transplantation, have been known to be related to the DTH mechanism (Kobayashi, Kaneda, & Kasama, 2001). These diseases are usually treated by immunosuppressants, which posses a strong anti-DTH activity (Allison, 2000).

The inhibitory effect of ESP-B4 on DNFB-induced DTH was illustrated in Fig. 3. The ear swelling was significantly increased in model group compared with that in control group ($p < 0.01$), indicating that DNFB-induced DTH model had been made successfully. The ear swelling was significantly decreased in mice treated with

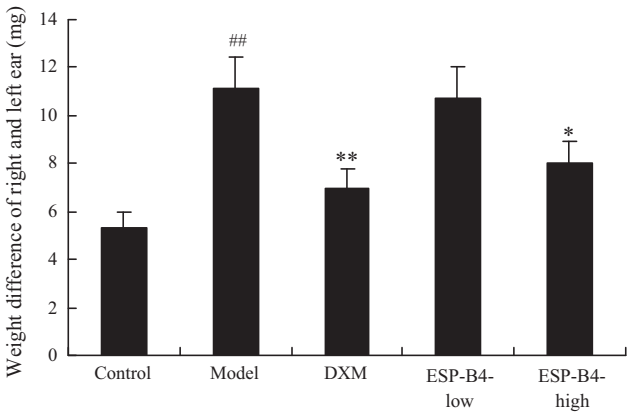

Fig. 3. Effects of ESP-B4 on the cell immunity of DNFB-treated mice evaluated by DTH. The antigen challenge was evaluated by measuring the weight difference between the right and left ear ($^{\#\#}p < 0.01$ vs. Control group, $^{**}p < 0.01$ vs. Model group, $^{*}p < 0.05$ vs. Model group).

the high dose of ESP-B4 (200 mg/kg) and standard drug DXM compared with that in model group ($p < 0.05$), respectively.

To determine whether ESP-B4 prevented DTH, we analyzed the histology of the mice ear skin (Fig. 4). Based on our HE staining results, no notable histological changes of the ear skin were observed, connective tissue was tightly packed without edema and infiltration of inflammatory cells in control group (Fig. 4A). However, monocytes, eosinophils and neutrophils were obviously increased, which have infiltrated into peribronchiole and perivascular connective tissue, leading to the tissue hypertrophy and edema (Fig. 4B). Compared with the model group, the tissue swelling had gone down a little, and the inflammatory cells infiltration had been decreased in the low dose of ESP-B4 (50 mg/kg) group (Fig. 4C). In the high dose of ESP-B4 (200 mg/kg) and the DXM groups (10 mg/kg), tissue hypertrophy was reduced much obviously, and only a few inflammatory cells infiltration were present (Fig. 4D and 4E). The results indicated that ESP-B4 played a significant immunosuppressive role.

T lymphocytes play a pivotal role in the pathogenesis of T cell-mediated autoimmune diseases and the chronic inflammatory disorders (Wu et al., 2010). Previous studies revealed that the polysaccharide extract of the stems of *E. sinica* could ameliorate T cell-mediated immune response (Kuang et al., 2011). So, T lymphocyte was focused on in this study to examine the activities of the compounds isolated. Effect of ESP-B4 on T cell response was studied using flow cytometric analysis. The effect of ESP-B4 on $CD3^+$, $CD4^+$ and $CD8^+$ counts was studied in DTH mice (Fig. 5). $CD4^+$ levels were higher in the model mice compared with that in the control mice ($p < 0.05$, Fig. 5A and C). $CD8^+$ levels were lower in the model mice compared with that in the control mice ($p < 0.05$, Fig. 5B and C). The ratio of $CD4^+/CD8^+$ was much higher in the model mice than that in the control mice ($p < 0.01$) (Fig. 5D). The ratio of $CD4^+/CD8^+$ in DTH mice serum was decreased by ESP-B4 in dose-dependent.

It is well-known that $CD4^+$ and $CD8^+$ are T helper (Th) and T cytotoxic (Tc) lymphocytes, respectively. Many researches have reported that the ratio of $CD4^+/CD8^+$ was higher in autoimmune and atopic diseases (Kang et al., 2009). The inhibitory effect of ESP-B4 on T cell functions was confirmed in T cell-mediated DTH response. These results suggest that ESP-B4 exhibited its inhibitory activity on DTH mice through down-regulating the function of over-activated macrophages and up-regulating that of the dysfunctional T lymphocytes from DTH mice. Further studies then elucidated the direct action of ESP-B4 on T cells. These observations indicated that ESP-B4 exerted immunosuppressive effect through its inhibition of T-cell activation and proliferation. Moreover, its immunosuppressive effect did not influence mice body weight (data not shown). Such characteristics of ESP-B4 are quite different from previous immunosuppressants and may be advantageous in the treatment of chronic rheumatic arthritis with an immune system disorder.

Cytokines play an important role in the immune system and are also potential targets for immunomodulation (Hill & Sarvetnick, 2002). It was clear that Th1 cells produce IL-2, IFN-γ, IL-12, and other cytokines when stimulated; and Th2 cells produced IL-4, IL-5, and IL-10 (Viallard et al., 1999; Yasui et al., 1998). IFN-γ plays a pivotal role in immunoinflammatory reactions. It can activate macrophages, which subsequently synthesize TNF-α and proinflammatory chemokines to maintain inflammation (Yoon, Jun, & Santamaria, 1998). In addition, high level of IL-4 plays a vital role in the development of many autoimmune diseases, including RA, EAE, and asthma (Samoilova, Horton, Hilliard, Liu, & Chen, 1998). In this study, the IL-2, IL-4 and IFN-γ concentrations in the serum were sig-

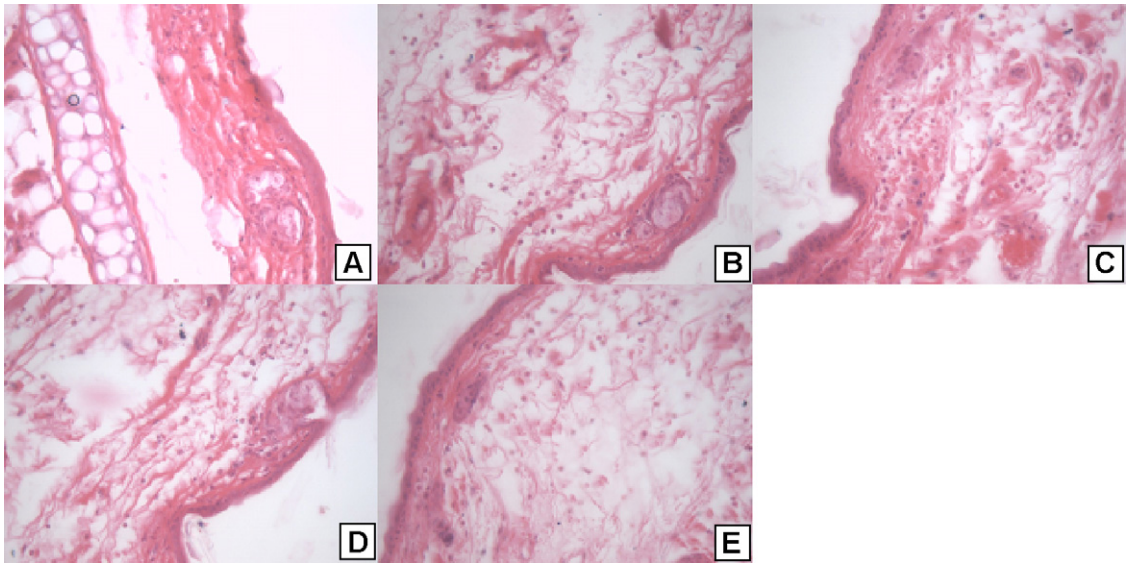

Fig. 4. Histological changes in right ear of mice at 24 h following elicitation with DNFB. A, Control Group; B, Model Group; C, ESP-B4-low Group; D, ESP-B4-high Group; E, DXM Group.

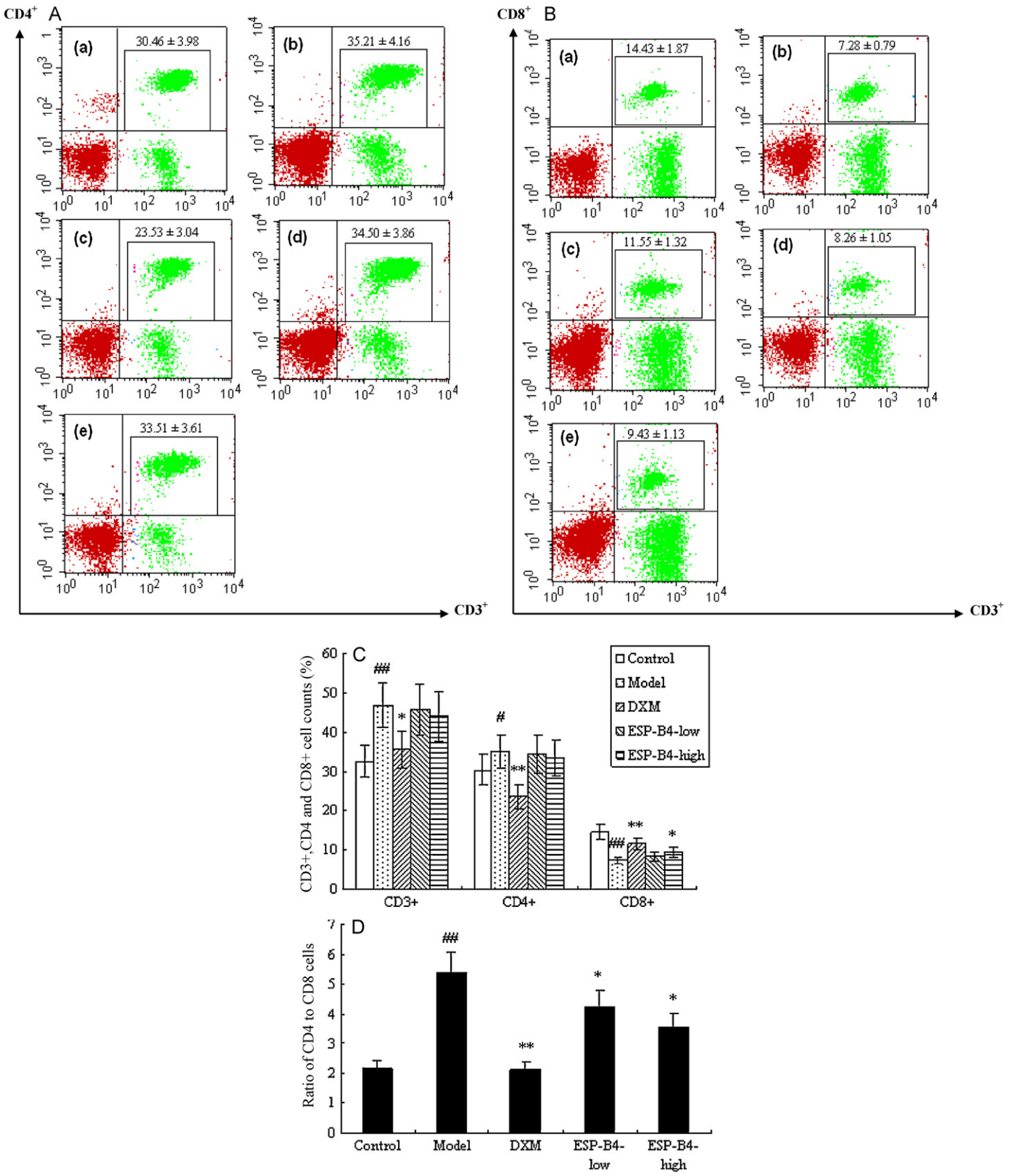

Fig. 5. (A) The density plot of ESP-B4 on $CD4^+$ T in $CD3^+$ T cells (%); (B) the density plot of ESP-B4 on $CD8^+$ T in $CD3^+$ T cells (%) in mice blood by flow cytometric analysis. (a) Control; (b) Model; (c) DXM; (d) ESP-B4-low; (e) ESP-B4-high; (C) effects of ESP-B4 on the $CD3^+$, $CD4^+$, $CD8^+$ cell counts; (D) ratio of $CD4^+/CD8^+$ cells in blood of DNFB-treated DTH mice ($^{\#}p < 0.05$ vs. Control group, $^{\#\#}p < 0.01$ vs. Control group, $^{*}p < 0.05$ vs. Model group, $^{**}p < 0.01$ vs. Model group).

nificantly ($p < 0.05$) higher in the model mice than that in the control mice (Fig. 6). The high dose of ESP-B4 significantly decreased IL-2 and IL-4 level in the serum ($p < 0.05$). The level of IFN-γ in high dose of ESP-B4 showed also a trend downward and was no significant difference between model group ($p > 0.05$). ESP-B4 inhibited IL-2, IL-4 and IFN-γ productions, which suggested a possible therapeutic role of ESP-B4 in the treatment of diseases associated with the synthesis/release of these cytokines.

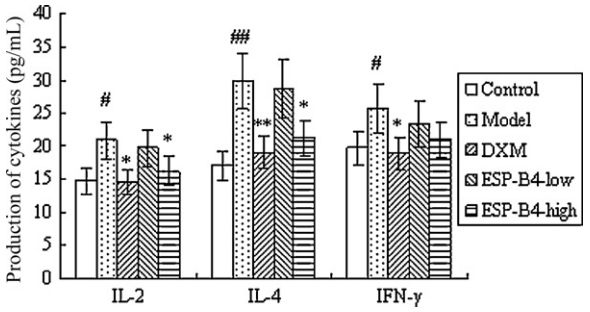

Fig. 6. Effects of ESP-B4 on the cytokines production in serum of DNFB-treated DTH mice ($^{\#}p < 0.05$ vs. Control group, $^{\#\#}p < 0.01$ vs. Control group, $^{*}p < 0.05$ vs. Model group, $^{**}p < 0.01$ vs. Model group).

4. Conclusion

Our data suggested that ESP-B4 from the stems of *E. sinica* possessed the following structure: the backbone consisted of the repeating disaccharide unit of [→4)-Gal*p*A-(1→2)-Rha*p*-(1→] as hairy region; side chains arabinan, arabinogalactan, a small proportion of terminal mannose, arabinose, xylose glucose and glucuronic acid were attached to the backbone through O-4 of some rhamnose residues and O-3 of partial galacturonic acid residues. Glc*p*A residues were not commonly found in pectic substances, although some terminal Glc*p*A residues were attached to O-2 and/or O-3 of 1,4-linked-Gal*p*A residues in the pectic polysaccharides of primary cell walls (Duan, Chen, Dong, Ding, & Fang, 2010). Immunological tests in vivo showed that ESP-B4 exhibits low toxicity and compelling immunosuppressive effects, which might be attributed to its inhibition of IL-2 and IL-4 levels in serum, and also effectively suppressed the ratio of $CD4^+/CD8^+$ in serum of T cell mediated DTH mice. We believe that the data warrant further evaluation of ESP-B4 as a possible therapeutic agent in the treatment of inflammatory and/or autoimmune diseases.

Acknowledgements

The authors wish to thank financial support for this study by the Major State Basic Research Development Program of China (973 Program 2006CB504708), State Key Creative New Drug Project of 12th Five-year Plan of China (2011ZX09102-006-01), National Natural Science Foundation of China (30973870), China Postdoctoral Science Foundation (20110490111), Heilongjiang Postdoctoral Science Foundation (LBH-Z10019) and Heilongjiang University of Chinese Medicine Doctor Innovative Foundation (B201002).

References

Allison, A. C. (2000). Immunosuppressive drugs: The first 50 years and a glance forward. *Immunopharmacology*, *47*, 63–83.

Bensadoun, A., & Weinstein, D. (1976). Assay of proteins in presence of interfering materials. *Analytical Biochemistry*, *54*, 484–489.

Cheng, R. M., Zhu, G. X., & Xu, Z. Y. (2001). Effect of different extracts from *Ephedra* on cell immunity. *Journal of Nanjing TCM University*, *17*, 234–236.

Comar, K. M., & Kirby, D. F. (2005). Herbal remedies in gastroenterology. *Journal of Clinical Gastroenterology*, *39*, 457–468.

Cui, S. W. (2005). *Food carbohydrates: Chemistry, physical properties, and applications*. Taylor & Francis Group: CRC Press.

Ding, L. L., Shi, R. S., Cui, J., Wang, S. C., & Wang, Z. T. (2006). Advances in research of chemical constituents and pharmacological activities of *Ephedra*. *China Journal of Chinese Materia Medica*, *31*, 1661–1664.

Dong, Q., Yao, J., Fang, J. N., & Ding, K. (2007). Structural characterization and immunological activity of two cold water extractable polysaccharides from Cistanche deserticola Y. C. Ma. *Carbohydrate Research*, *342*, 1343–1349.

Duan, J. Y., Chen, V. L., Dong, Q., Ding, K., & Fang, J. N. (2010). Chemical structure and immunoinhibitory activity of a pectic polysaccharide containing glucuronic acid from the leaves of *Diospyros kaki*. *International Journal of Biological Macromolecules*, *46*, 465–470.

Ghosh, K., Chandra, K., Roy, S. K., Mondal, S., Maiti, D., Das, D., et al. (2008). Structural investigation of a polysaccharide (Fr. I) isolated from the aqueous extract of an edible mushroom, Volvariella diplasia. *Carbohydrate Research*, *343*, 1071–1078.

He, L., Yin, N., Cheng, J. W., Wu, X. Q., Jiang, J. X., & Song, X. L. (2009). Structural features of a new heteropolysaccharide from the fruit bodies of *Melia azedarach* and its effect on cytotoxic activity. *Fitoterapia*, *80*, 399–403.

Hill, N., & Sarvetnick, N. (2002). Cytokines: Promoters and dampeners of autoimmunity. *Current Opinion in Immunology*, *14*, 791–797.

Kang, H., Choi, T. W., Ahn, K. S., Lee, J. Y., Ham, I. H., Choi, H. Y., et al. (2009). Upregulation of interferon-γ and interleukin-4, Th cell-derived cytokines by So-Shi-Ho-Tang (Sho-Saiko-To) occurs at the level of antigen presenting cells, but not $CD4^+$ T cells. *Journal of Ethnopharmacology*, *123*, 6–14.

Kobayashi, K., Kaneda, K., & Kasama, T. (2001). Immunopathogenesis of delayed-type hypersensitivity. *Microscopy Research and Technique*, *53*, 24–245.

Kuang, H. X., Xia, Y. G., Yang, B. Y., Wang, Q. H., & Wang, Y. H. (2011). Screening and comparison of the immunosuppressive activities of polysaccharides from the stems of *Ephedra sinica* Stapf. *Carbohydrate Polymers*, *83*, 787–795.

Li, J. W., Fan, L. P., & Ding, S. D. (2011). Isolation, purification and structure of a new water-soluble polysaccharide from *Zizyphus jujuba cv. Jinsixiaozao*. *Carbohydrate Polymers*, *83*, 477–482.

Mondal, S., Chandra, K., Maiti, D., Ojha, A. K., Das, D., Roy, S. K., et al. (2008). Chemical analysis of a new fucoglucan isolated from an edible mushroom, Termitomyces robustus. *Carbohydrate Research*, *343*, 1062–1070.

Ojha, A. K., Maiti, D., Chandra, K., Mondal, S., Roy, D. D. S. K., Ghosh, K., et al. (2008). Structural assignment of a heteropolysaccharide isolated from the gum of *Cochlospermum religiosum* (Katira gum). *Carbohydrate Research*, *343*, 1222–1231.

Qiao, D. L., Liu, J., Ke, C. L., Sun, Y., Ye, H., & Zeng, X. X. (2010). Structural characterization of polysaccharides from *Hyriopsis cumingii*. *Carbohydrate Polymers*, *82*, 1184–1190.

Samoilova, E. B., Horton, J. L., Hilliard, B., Liu, T. S., & Chen, Y. (1998). IL-6 deficient mice are resistant to experimental autoimmune encephalomyelitis: Roles of IL-6 in the activation and differentiation of autoreactive T cells. *The Journal of Immunology*, *161*, 6480–6486.

Sun, L. W., Feng, K., Jiang, R., Chen, J. Q., Zhao, Y., Ma, R., et al. (2010). Water-soluble polysaccharide from *Bupleurum chinense* DC: Isolation, structural features and antioxidant activity. *Carbohydrate Polymers*, *79*, 180–183.

Tong, H. B., Liang, Z. Y., & Wang, G. Y. (2008). Structural characterization and hypoglycemic activity of a polysaccharide isolated from the fruit of *Physalis alkekengi* L. *Carbohydrate Polymers*, *71*, 316–323.

Viallard, J. F., Pellegrin, J. L., Ranchin, V., Schaeverbeke, T., Dehais, J., Boursier, M. L., et al. (1999). Th1 (IL-2, interferon-gamma (IFN-γ)) and Th2 (IL-10, IL-4) cytokine production by peripheral blood mononuclear cells (PBMC) from patients with systemic lupus erythematosus (SLE). *Clinical Experimental Immunology*, *115*, 189–195.

Wu, C. R., Jiang, X., He, S. T., Yang, B., Hu, J. Z., & Cai, R. (2010). Effects of QWBZP on T-cell subsets and their cytokines in intestinal mucosa of HRV infection suckling mice. *Journal of Ethnopharmacology*, *131*, 130–134.

Xia, Y. G., Kuang, H. X., Yang, B. Y., Wang, Q. H., Liang, J., Sun, Y. P., et al. (2011). Optimum extraction of acidic polysaccharides from the stems of *Ephedra sinica* Stapf by Box–Behnken statistical design and its anti-complement activity. *Carbohydrate Polymers*, *84*, 282–291.

Xia, Y. G., Liang, J., Yang, B. Y., Wang, Q. H., & Kuang, H. X. (2010). Identification of two cold water-soluble polysaccharides from the stems of *Ephedra sinica* Stapf. *Chinese Medicine*, *1*, 63–68.

Xia, Y. G., Wang, Q. H., Liang, J., Yang, B. Y., Li, G. Y., & Kuang, H. X. (2011). Development and application of a rapid and efficient HPCE method coupled with correction factors for determination of monosaccharide composition of acidic heteropolysaccharides from *Ephedra sinica*. *Phytochemical Analysis*, *22*, 103–111.

Yasui, D. H., Genetta, T., Kadesch, T., Williams, T. M., Swain, S. L., Tsui, L. V., et al. (1998). Transcriptional repression of the IL-2 gene in Th cells by ZEB. *The Journal of Immunology*, *160*, 4433–4440.

Yin, Y., Gong, F. Y., Wu, X. X., Sun, Y., Li, Y. H., Chen, T., et al. (2008). Anti-inflammatory and immunosuppressive effect of flavones isolated from *Artemisia vestita*. *Journal of Ethnopharmacology*, *120*, 1–6.

Yoon, J. W., Jun, H. S., & Santamaria, P. (1998). Cellular and molecular mechanisms for the initiation and progression of beta cell destruction resulting from the collaboration between macrophages and T cells. *Autoimmunity*, *27*, 109–122.

Zhu, M. Y., Mo, J. G., He, C. S., Xie, H. P., Ma, N., & Wang, C. J. (2010). Extraction, characterization of polysaccharides from lycium barbarum and its effect on bone gene expression in rats. *Carbohydrate Polymers*, *80*, 672–676.